Ultrafast Electron Relaxation in Superconducting $Bi_2Sr_2CaCu_2O_{8+\delta}$ by Time-Resolved Photoelectron Spectroscopy

L. Perfetti,[1] P. A. Loukakos,[1] M. Lisowski,[1] U. Bovensiepen,[1] H. Eisaki,[2] and M. Wolf[1]

[1]*Fachbereich Physik, Freie Universität Berlin, Arnimallee 14, 14195 Berlin, Germany*

[2]*AIST Tsukuba Central 2, 1-1-1 Umenzono, Tsukuba, Ibaraki 305-8568, Japan*

(Received 18 April 2007; published 9 November 2007)

Time-resolved photoelectron spectroscopy is employed to study the dynamics of photoexcited electrons in optimally doped $Bi_2Sr_2CaCu_2O_{8+\delta}$ (Bi-2212). Hot electrons thermalize in less than 50 fs and dissipate their energy on two distinct time scales (110 fs and 2 ps). These are attributed to the generation and subsequent decay of nonequilibrium phonons, respectively. We conclude that 20% of the total lattice modes dominate the coupling strength and estimate the second momentum of the Eliashberg coupling function $\lambda\Omega_0^2 = 360 \pm 30$ meV^2. For the typical phonon energy of copper-oxygen bonds ($\Omega_0 \simeq$ 40–70 meV), this results in an average electron-phonon coupling $\lambda < 0.25$.

DOI: 10.1103/PhysRevLett.99.197001 PACS numbers: 74.25.Jb, 74.25.Kc, 74.62.Yb, 74.72.Hs

Since their first discovery in 1986, the high temperature superconductors (HTSCs) have always been the subject of debates. After 20 years of investigation, the mechanism leading to the Cooper pairs is still under discussion. The small isotope effect of optimally doped samples [1], the *d*-wave symmetry of the superconducting gap [2], and the proximity of an antiferromagnetic phase shade doubts on a phonon mediated pairing mechanism. For this reason, a better knowledge of the electron-phonon (*e*-ph) interaction would be essential to understand the origin of superconductivity. Despite it, the common experimental techniques could provide only a rough estimate of the average strength of *e*-ph coupling [3]. Most of the reported values refer to specific lattice modes [4] or electronic states that have been detected [5]. Furthermore, different interpretations of the same data have often generated plausible but conflicting scenarios. As an example, angle resolved photoelectron spectroscopy (ARPES) measures the quasiparticle scattering due to coupled bosons [6] but does not allow for a clear distinction between phonon and spin excitations [2]. These controversies call for new and complementary methods that could provide additional information on the electron-phonon coupling.

The investigation of nonequilibrium states by femtosecond laser spectroscopy is a powerful technique to observe the *e*-ph scattering directly in the time domain. Indeed, an ultrashort light pulse can selectively excite the electrons of a metal without perturbing the underlying lattice. After the spin and charge fluctuations of the photoexcited electrons have thermalized, the rate of energy transfer from hot electrons to the lattice is governed by the electron-phonon interaction [7]. Some all-optical experiments already followed this approach to extract the coupling strength of HTSCs [8,9]. However, these attempts face the inherent problem of connecting the transient dielectric properties to the electron dynamics [10–12]. Time-resolved ARPES circumvents the problem by directly probing the electronic states and their occupation [13,14]. As sketched in Fig. 1(a), a pump pulse centered at 1.5 eV excites the sample while a 6 eV probe generates photoelectrons after a variable time delay τ. In the following, this technique is employed to investigate optimally doped $Bi_2Sr_2CaCu_2O_{8+\delta}$ (Bi-2212). The observed cooling time of hot electrons indicates that the average interaction strength between electrons and phonons is weak. Moreover, the observation of an energy bottleneck suggests that only a minor subset of the total phonon modes contributes to the coupling. We attribute this finding to the strong anisotropy of the *e*-ph interaction and to the presence of phonon branches with inferior coupling strength.

In our experiment, single crystals of optimally doped $Bi_2Sr_2CaCu_2O_{8+\delta}$ (transition temperature of 91 K) are cleaved in ultrahigh vacuum (5×10^{-11} mbar). The sample is excited by 50 fs pulses at 1.5 eV photon energy with

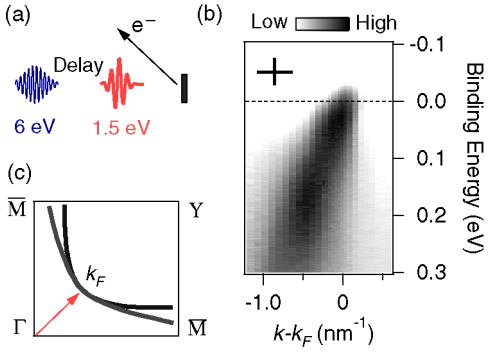

FIG. 1 (color online). (a) Sketch of the time-resolved ARPES experiment. An infrared pulse excites the sample while a delayed UV pulse generates the photoelectrons. (b) Photoelectrons intensity map acquired along the nodal direction (lattice temperature $T_l = 30$ K). Vertical and horizontal bars display the energy and angular resolution, respectively. (c) Bonding and antibonding Fermi surfaces of Bi2212 in the reciprocal space. The arrow (red) marks the nodal vector k_F.

30 kHz repetition rate and a fluence of $\simeq 100\ \mu J/cm^2$. No multiphoton photoemission from the pump beam is observed. The transient electron distribution is probed by 80 fs pulses at 6 eV, whereby the photoemitted electrons are analyzed normal to the surface in a time of flight spectrometer with energy resolution of 10 meV and acceptance angle of $\pm 3°$.

The equilibrium state at lattice temperature $T_l = 30$ K is probed by blocking the pump beam and collecting the photoelectron intensity at different emission angles. Figure 1(b) shows the electronic band crossing the Fermi level along the nodal direction while Fig. 1(c) depicts the crossing wave vector k_F in the first Brillouin zone of Bi-2212. Here, the concepts of Fermi surface and quasiparticle hold even in the superconducting phase [15] and for underdoped samples [16]. According to high resolution measurements, the interaction of the quasiparticles with boson modes determines a kink in the electronic dispersion [6]. The map of Fig. 1(b) does not resolve such fine structures because of the large acceptance angle of the analyzer and the broad bandwidth of the probe pulses. On the other hand, the photoelectrons emitted by the 80 fs probe pulse reveal the electronic thermalization and energy relaxation time.

Figure 2(a) compares ARPES spectra collected along the nodal direction before and just after the absorption of the pump pulse. Since the optical coherence of photoexcited Bi-2212 is lost after a few femtoseconds [17], we assign the pump- induced signal to the transient population of photoexcited states. The large spectral changes near the Fermi level thus originate from the nonequilibrium distribution $f(\omega, \tau)$. The logarithmic plot in Fig. 2(b) compares the spectrum acquired at $\tau = 0$ with the one expected for thermalized electrons. We observe that the deviations do not exceed 1% of the total counts and conclude that $f(\omega, \tau)$ converges to a Fermi-Dirac distribution within the duration of the pump pulse. This fast thermalization is due to the large electron-electron interaction existing in HTSCs. Figure 2(c) displays spectra acquired at different pump-probe delays. We extract the temporal evolution of the electronic temperature T_e by fitting the spectra with an exponential function covering the energy range $-300\ \text{meV} < \omega < -50\ \text{meV}$. The assumption of a thermalized population is verified by evaluating the electronic energy E from the ω-weighted area of the hot electron's tail. Above the transition temperature, the electronic specific heat of optimally doped Bi-2212 is proportional to T_e [18]. Therefore, the electronic temperature that describes the photoexcited spectrum of Fig. 2(b) should scale as $\sqrt{E}$. Figure 3(a) show that the deviations from the scaling law $T_e \propto \sqrt{E}$ are always below the experimental uncertainties.

Figure 3(b) displays the temporal evolution of $T_e(\tau)$ until 18 ps. Before excitation, i.e., negative delays, the electrons and phonons are in equilibrium at $T_e = T_l = 30$ K. During the absorption of the pump pulse, the electronic temperature increases by $\Delta T_e^{\alpha} = 740$ K. Con-

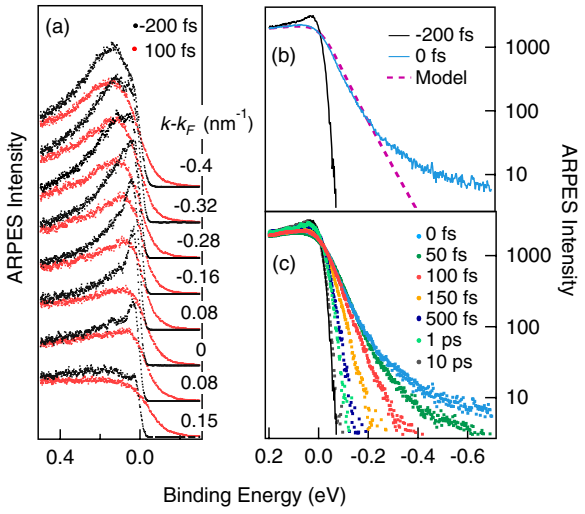

FIG. 2 (color online). (a) Time-resolved ARPES spectra acquired 200 fs before (black dots) and 100 fs after [gray (red) dots] the arrival of the pump pulse ($T_l = 30$ K). (b) Time-resolved ARPES spectra acquired at $\tau = 0$ fs [gray (azure) line] and at $\tau = -200$ fs (black line). Hypothetical spectrum of an electronic system that has fully thermalized at $T_e = 770$ K [dashed (violet) line]. (c) Logarithmic plot of the k_F spectrum collected at several pump-probe delays.

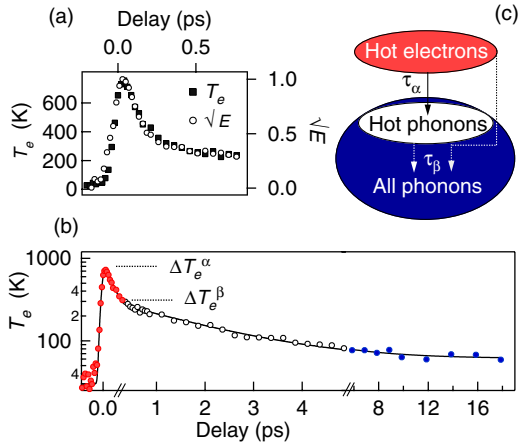

FIG. 3 (color online). (a) The electronic temperature $T_e(\tau)$ is compared to the square root of the excess energy $\sqrt{E}(\tau)$. The function $\sqrt{E}$ is normalized to the maximum value. (b) Logarithmic plot of the electronic temperature ($T_l = 30$ K). Three temporal windows indicate different cooling processes. The maximum increase of electronic temperature is marked by ΔT_e^{α}. Hot electrons and hot phonons converge to $T_l + \Delta T_e^{\beta}$ at $\tau = 3\tau_{\alpha} = 330$ fs. When $\tau > 3\tau_{\beta} = 6$ ps, the electrons and phonons reach local equilibrium. The solid line is the fitting result of the coupled Eqs. (1)–(3). (c) Sketch of the energy transfer during the relaxation process. Hot electrons generate hot phonons with characteristic time τ_{α}, while hot phonons dissipate their energy on a time scale $\tau_{\beta} \gg \tau_{\alpha}$.

versely, the lattice temperature is still near the equilibrium value. As shown by Figs. 3(a) and 3(b), the electronic temperature displays a drop to 300 K in ≃100 fs, which is followed by a decay lasting several picoseconds. The slower relaxation has not been observed in usual metals but has been reported in anisotropic materials as graphite [19]. Our interpretation of the observed dynamics is sketched in the diagram of Fig. 3(c). We assume that charge and spin fluctuations are thermalized and can be lumped in a unique bath with specific heat C_e. Ballistic transport of hot electrons out of the surface [20] is neglected because of the quasi-two-dimensional layered structure of Bi-2212. For the phonons we consider two subsets: (i) a limited number of modes, which interact more strongly with the electrons, and (ii) a complementary subset of nearly noninteracting modes. Electrons transfer energy to the phonons that are more strongly coupled with a characteristic time $\tau_\alpha =$ 110 fs. Because of their small specific heat, this small subset of the total phonons acquires an effective temperature $T_p > T_l$. Already after $\tau = 3\tau_\alpha = 330$ fs, the hot electrons and hot phonons reach a common temperature $T_p \simeq T_e = T_l + \Delta T_e^\beta = 300$ K, and the dynamics of hot electrons and hot phonons become similar. The electronic cooling can still proceed due to a residual scattering with the cold lattice modes. Moreover, we expect that hot phonons dissipate their energy by means of anharmonic decay. The relaxation by anharmonic cooling and scattering with cold phonons takes place with time constant $\tau_\beta =$ 2 ps. After $3\tau_\beta$, the sample surface is in local equilibrium at $T_l = 60$ K. Heat diffusion from the surface to the bulk leads to the recovery of $T_l = 30$ K within several nanoseconds.

Figure 3(c) sketches the two stages of the energy relaxation. The existence of a cooling dynamics with two different time scales $\tau_\beta \gg \tau_\alpha$ implies a sudden reduction of energy flow, which is often referred to as bottleneck. In previous work, the energy bottleneck has been ascribed to the opening of a superconducting gap [21]. We do not exclude that an instability of the Fermi surface may further reduce the cooling rate. However, the bottleneck occurs already at $T_e^\beta = 300$ K, therefore well above the superconducting transition temperature. Moreover, it is well established that hot phonons arise even in gapless compounds [19]. The same instance holds also for optimally doped Bi-2212. Figure 4 shows the evolution of electronic temperature when the sample is originally in the superconducting phase ($T_l = 30$ K) and in the metallic phase ($T_l = 300$ K). The energy bottleneck is clearly visible in both cases.

Quantitative insight on the relative number and coupling strength of the nonequilibrium phonons is obtained by solving an extended version of the two temperature model. The rate of energy transfer from electrons to phonons is related to the Eliashberg coupling function $\alpha^2F(\Omega)$ through the integral $\int \Omega^2\alpha^2F(n_e - n_p)d\Omega$ [7]. The distributions n_e and n_p are $(e^{\Omega/k_bT_e} - 1)^{-1}$ and $(e^{\Omega/k_bT_p} - 1)^{-1}$, respectively. We approximate the phonons spectrum by an Einstein model $F(\Omega) = \delta(\Omega - \Omega_0)$. These modes are coupled to the electrons through the dimensionless parameter $\lambda = 2\int \Omega^{-1}\alpha^2F d\Omega$. The functions $T_e(\tau)$, $T_p(\tau)$, and $T_l(\tau)$ satisfy the rate equations:

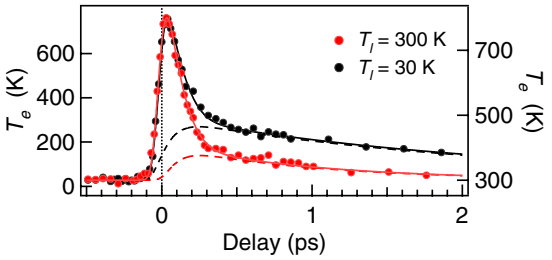

FIG. 4 (color online). Temporal evolution of electronic temperature for $T_l = 30$ K (black marks, left axis) and $T_l = 300$ K (red marks, right axis). The solid and dashed lines are numerical simulations of the hot electron and hot phonon temperature, respectively.

$$\frac{\partial T_e}{\partial \tau} = -\frac{3\lambda\Omega_0^3}{\hbar\pi k_B}\frac{n_e - n_p}{T_e} + \frac{P}{C_e}, \tag{1}$$

$$\frac{\partial T_p}{\partial \tau} = \frac{C_e}{C_p}\frac{3\lambda\Omega_0^3}{\hbar\pi k_B}\frac{n_e - n_p}{T_e} - \frac{T_p - T_l}{\tau_\beta}, \tag{2}$$

$$\frac{\partial T_l}{\partial \tau} = \frac{C_p}{C_l}\frac{T_p - T_l}{\tau_\beta}. \tag{3}$$

The system is excited by a Gaussian pulse P with FWHM of 50 fs and energy density of 12 J/cm^3. The specific heat of electrons, hot phonons, and rest of the lattice are $C_e = \gamma T_e$, $C_p = 3f\Omega_0\frac{\partial n_p}{\partial T_p}$, and $C_l = 3(1-f)\Omega_0\frac{\partial n_p}{\partial T_p}$, respectively. Here, the parameter f indicates the fraction of total modes that are more strongly coupled. Electron-phonon scattering with the $(1-f)$ lattice modes that are more weakly coupled barely contributes to the temporal evolution of T_e and has been therefore neglected. The decay time τ_β describes the anharmonic decay of hot phonons. In agreement with the expected behavior, τ_β is larger at 30 K than at 300 K. We extract the coupling strength and relative size of the hot phonons subset by fitting the measured T_e with the numeric solution of Eq. (1). The resulting

TABLE I. Fitting parameters of the model described by Eqs. (1)–(3). The smallest and highest values of f and $\lambda\Omega_0^2$ correspond to the choice $\Omega_0 = 40$ meV and $\Omega_0 = 70$ meV, respectively.

T_l	f	$\lambda\Omega_0^2$ (meV^2)	τ_β (ps)
30 ± 10	0.13–0.25	300–380	2 ± 0.1
300 ± 10	0.18–0.25	340–380	0.9 ± 0.1

parameters vary slightly for $40\ \text{meV} \leq \Omega_0 \leq 70\ \text{meV}$. Table I reports minimum and maximum values of f and $\lambda\Omega_0^2$. The best estimate $\lambda\Omega_0^2 = 360 \pm 30\ \text{meV}^2$ supports a weak electron-phonon coupling. Indeed, several electron spectroscopy experiments indicate that copper-oxygen modes with quantum energy of 40–70 meV dominate the electron-phonon coupling [22,23]. If we assume that the mean phonon energy Ω_0 is larger than 40 meV, the average electron-phonon coupling λ does not exceed 0.25.

Obviously, the experimental determination of $\lambda\Omega_0^2$ offers an important term of comparison to theoretical calculations. Indeed, $\lambda\Omega_0^2 = 2\int \Omega\alpha^2 F d\Omega$ can be directly evaluated from the Eliashberg coupling function [7]. We are not aware of calculations of the electron-phonon coupling in Bi-2212. However, our results are in excellent agreement with density functional theory calculations of the parent compound $YBa_2Cu_3O_7$ [24]. The estimated zero and second momenta of α^2F are $\lambda = 0.27$ and $\lambda\Omega_0^2 = 380\ \text{meV}^2$, respectively. This coupling is rather small if compared with the $\lambda = 0.61$ and $\lambda\Omega_0^2 = 2.8\ \text{eV}^2$ [25] that has been calculated for MgB_2.

The second point of interest regards the nature of the energy bottleneck. The value $f \simeq 0.2$ implies that 80% of the phonon modes have very weak interaction with the electrons. Two reasons can explain this finding: (i) only a few branches are significantly coupled, and (ii) the interaction is highly anisotropic. Nowadays, there is a general agreement on both issues. ARPES experiments on $Bi_2Sr_2Ca_{0.92}Y_{0.08}Cu_2O_{8+\delta}$ show that quasiparticle scattering strongly depends on the electronic wave vector [22]. Moreover, inelastic neutron scattering measurements of $La_{8-\delta}Sr_\delta CuO_4$ report a wave vector dependent softening of the breathing and half-breathing mode [26] with increasing doping level. In agreement with these experimental results, also first principles calculations predict an electron-phonon coupling that strongly depends on the branch and wave vector of the mode [24,27]. Finally, the electron-phonon coupling of Bi-2212 may also be spatially inhomogeneous. Recent scanning tunneling spectroscopy (STS) experiments reveal a strong modulation of the electronic density at the nanometer scale [28]. The short range order of the electrons' density could modulate the local strength of the electron-phonon interaction [23], favoring a selective coupling of some modes with respect to others.

In conclusion, we investigated the energy relaxation of excited electrons in Bi2212. The electronic temperature displays a fast initial drop within $\simeq$200 fs, which is followed by a slower decay lasting several picoseconds. This finding implies that 20% of the phonons is driven out of equilibrium, whereas the major part of lattice modes are almost uncoupled to the electrons. Furthermore, time-resolved ARPES provides a quantitative evaluation of the electron-phonon interaction [7]. We extract the second momentum of the Eliashberg coupling function from the dynamics of the hot electrons. The best value $\lambda\Omega_0^2 = 360\ \text{meV}^2$, together with the mean phonon frequency derived by ARPES [22] and STS [23], suggests that the average electron-phonon coupling of optimally doped $Bi_2Sr_2CaCu_2O_{8+\delta}$ is weak. This finding argues against a pairing mechanism that is purely mediated by phonons. On the other hand, it does not exclude that some strongly coupled lattice modes cooperate with other interactions to stabilize the superconducting phase.

We acknowledge H. Glawe and A. Floris for useful discussions, K. H. Benneman for critically reading the manuscript, and K. Lüders for characterizing the samples. This work has been supported by the Deutsche Forschungsgemeinschaft, and a Marie Curie Action (Contract No. 514954).

[1] B. Batlogg *et al.*, Phys. Rev. Lett. **58**, 2333 (1987).
[2] A. Damascelli, Z. Hussain, and Z.-X. Shen, Rev. Mod. Phys. **75**, 473 (2003).
[3] M. Gurvitch and A. T. Fiory, Phys. Rev. Lett. **59**, 1337 (1987).
[4] C. Thomsen *et al.*, Solid State Commun. **75**, 219 (1990).
[5] W. Meevasana *et al.*, Phys. Rev. Lett. **96**, 157003 (2006).
[6] J. D. Koralek *et al.*, Phys. Rev. Lett. **96**, 017005 (2006).
[7] P. B. Allen, Phys. Rev. Lett. **59**, 1460 (1987).
[8] S. D. Brorson *et al.*, Solid State Commun. **74**, 1305 (1990).
[9] S. V. Chekalin *et al.*, Phys. Rev. Lett. **67**, 3860 (1991).
[10] J. Demsar *et al.*, Phys. Rev. Lett. **82**, 4918 (1999).
[11] R. A. Kaindl *et al.*, Science **287**, 470 (2000).
[12] G. P. Segre *et al.*, Phys. Rev. Lett. **88**, 137001 (2002).
[13] L. Perfetti *et al.*, Phys. Rev. Lett. **97**, 067402 (2006).
[14] R. Haight *et al.*, Phys. Rev. Lett. **54**, 1302 (1985).
[15] H. Ding *et al.*, Phys. Rev. Lett. **74**, 2784 (1995).
[16] D. S. Marshall *et al.*, Phys. Rev. Lett. **76**, 4841 (1996).
[17] W. Nessler *et al.*, Phys. Rev. Lett. **81**, 4480 (1998).
[18] J. W. Loram *et al.*, Physica (Amsterdam) **341C**, 831 (2000).
[19] T. Kampfrath *et al.*, Phys. Rev. Lett. **95**, 187403 (2005).
[20] E. Knoesel *et al.*, Phys. Rev. B **57**, 12812 (1998).
[21] V. V. Kabanov *et al.*, Phys. Rev. Lett. **95**, 147002 (2005).
[22] T. Cuk *et al.*, Phys. Rev. Lett. **93**, 117003 (2004).
[23] J. Lee *et al.*, Nature (London) **442**, 546 (2006).
[24] K. P. Bohnen *et al.*, Europhys. Lett. **64**, 104 (2003).
[25] H. J. Choi *et al.*, Phys. Rev. B **66**, 020513(R) (2002).
[26] L. Pintschovius, Phys. Status Solidi (b) **242**, 30 (2005).
[27] S. Y. Savrasov *et al.*, Phys. Rev. Lett. **77**, 4430 (1996).
[28] K. McElroy *et al.*, Science **309**, 1048 (2005).